



# THE SIMPLE WAY TO BUILD A GEOELECTRICAL INSTRUMENT

Risky Martin Antosia

Department of Geophysical Engineering, Institut Teknologi Sumatera, South Lampung, Indonesia

E-Mail: [martin.antosia@tg.itera.ac.id](mailto:martin.antosia@tg.itera.ac.id)

## ABSTRACT

Many researchers have actively applied geoelectrical equipment for some studies. Similar instruments had been developed to achieve their purposes; to reduce the high cost of commercial equipment. In this study, a geoelectrical system was introduced with the advantages of a low-cost, simple design, and easy to assemble. The DC power module of the instrument employed the isolated DC to DC converter module. It implemented nine converter modules to produce an output voltage of about 500 V with an output power of about 200 W. The measurement result presented a confidence level greater than 95%, both in a laboratory using an equivalent circuit; and in a field applying a 1-D geoelectrical method to identify the aquifer. The result of actual field data interpreted that the aquifer's estimated depth matches the depth of nearby groundwater wells. Then from the field testing, the built instrument had a close outcome to the commercial one.

**Keywords:** DC power, equivalent circuit, geoelectrical equipment, Isolated DC to DC converter.

## 1. INTRODUCTION

Geoelectrical equipment had been actively applied for groundwater reservoir exploration [1-3], engineering site investigation [4, 5], and bedrock identification [6, 7]. It was also used for the rock sample measurement [8] and soil resistivity analysis [9-16] for laboratory experiments; and also, the analysis in the field site [17, 18]. There was a comparative study of some commercial geoelectrical instruments for agriculture purposes [19].

The instrument is used not only by the researchers but also by the university students, especially in earth science and the related fields. There are about 90 earth programs in some universities in one of the developing countries, including earth science [20], geophysics [21], geology [22], and geography [23]. So, many researchers have developed or constructed the geoelectrical system to support those needs. Some studies had built digital systems using a microcontroller/embedded system [2, 6, 8, 11, 12, 14, 16, 18, 24, 25] and developed the automatic multichannel system with control software on a computer [10, 15, 26]. A simple design consisted of a DC (Direct Current) power module and two commercial digital multimeters [4, 5].

Based on those built systems, one of the system's main parts is the electrical power driven by a 12 V DC. The previous studies constructed two electrical power modules: the current and voltage sources. Indarto *et al.* [24] developed the current source with the constant output of 0.1 mA and one mA, and Setiadi [14] extended it with the output current of 1-10 mA. In comparison, some research had been carried out to develop the voltage source with a different method and targeted output voltage. At the same time, Meraz *et al.* [13] built the AC (Alternating Current) power with adjustable frequency. Then, Acho *et al.* [9] created the DC to AC converter with the output voltage of 230 V at a constant frequency. The author thinks that the system is not simple to be built by the earth science and engineering students because it needs more time to study before implementing it.

In contrast, there were four classifications of the DC voltage source module. First the module with an output voltage under 120 V [10, 12]; the output of 250 V [5] and 500 V [6]; and the last is the module with a target output voltage of 1,000-1,200 V [1, 16]. There were some methods to build a DC power module. Some studies have developed the module using a boost converter circuit [2, 6, 10]. Then, the Cockroft-Walton method, known as a voltage multiplier circuit, was implemented by Ahmad *et al.* [1] to create the module that enhances the AC voltage from the 230 V into a higher voltage and then converted it to the DC voltage. At the same time, the researchers constructed the module using the inverter circuit to convert the 12 V DC into the 220 V AC and then applied a rectifier circuit to transform it into the DC voltage [4, 5]. This system is more applicable for the students than the current source system.

Those built systems referred to much commercial equipment that uses the DC voltage source system. They have an output voltage above 300 V [27-30]. Although the commercial systems are available and can be shipped worldwide, Ahmad *et al.* [1] and Olanrewaju *et al.* [4] said their price is high. They need to be imported from the manufacturer's country to the user's country with a high shipping fee and duty tax [4]. It might be one of the reasons why the researchers had constructed their instruments to carry out some studies with a limited budget in their home country, like Ahmad *et al.* [1] that built the geoelectrical equipment using local components with a production cost of about 500 USD.

Therefore, this study proposes a simple system that refers to Olanrewaju *et al.* [4] and Urang *et al.* [5] with another approach to construct the DC power module with an output of about 500 V. For the objective of the education needs, the local components will also be used to achieve a low cost of equipment production. So that it is ready to use, simple testing will be required, including a case study with actual data acquisition in the field.



## 2. MATERIALS AND METHODS

Telford *et al.* [31] introduced a basic geoelectrical equipment schematic. It consists of a primary system and accessories. Figure-1 shows that the central system is an electrical power module, an amperemeter, and a voltmeter. Then, the additions include four electrodes ( $C_1$ ,  $C_2$ ,  $P_1$ , and  $P_2$ ) and wires (cables) connect the electrodes to the primary system.

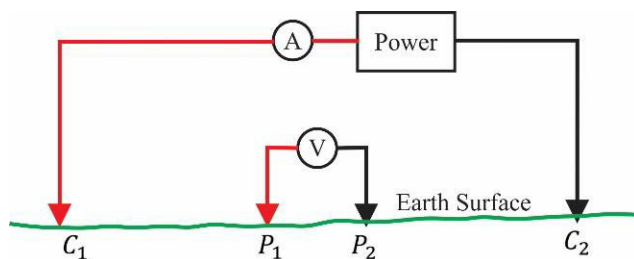


**Figure-1.** Basic schematic of geoelectrical equipment (modified from Telford *et al.* [31]).

In the previous explanation, most of the electrical power modules in a geoelectrical instrument employed the DC voltage source system (the DC power module). There are two other approaches to constructing the DC power module. First, the module uses batteries connection in series, as shown in Figure-2. The symbols ( $E_1$ ,  $E_2$ , and  $E_n$ ) are the battery voltage of the first, the second, and the n-th, respectively. Then, the total battery voltage ( $E_T$ ) can be obtained with the following equation

$$E_T = E_1 + E_2 + \dots + E_n \quad (1)$$

If each battery has the same voltage of  $E$ , like the statement below

$$E_1 = E_2 = \dots = E_n = E \quad (2)$$

the total voltage in Eq. (1) will be

$$E_T = N_b E \quad (3)$$

with  $N_b$  is the number of the batteries. Accordingly, if each battery has a voltage ( $E$ ) of 12 V and the total targeted voltage ( $E_T$ ) is 500 V, the number of batteries ( $N_b$ ) is about 42 pieces.

A common purpose uses an automotive rechargeable battery. According to [32], the minimum dimension of a 12 V battery is 97 x 45 x 53 mm and weighs about 0.59 kg. By connecting in series up to 42 batteries, one of the dimension possibilities will be 582 x 294 x 53 mm (still affordable) with a weight of about 25

kg. This system is straightforward, but the weight is hefty. If a 12 V battery has a minimum price of around 15 USD [32], the battery only will cost 630 USD (later, it will be compared to the next system). Because of the weight, this study will not implement this method.

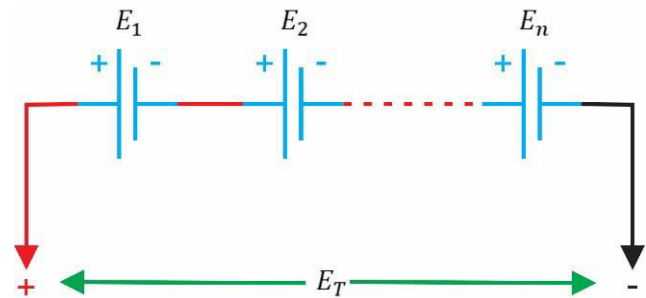


**Figure-2.** DC power circuit comes from batteries connection in series.

In this study, the construction of the DC power module will employ the second approach. It uses some isolated DC to DC converter modules connected in series. The module converts a 12 V DC to a higher DC voltage, with the input ground being different from the output ground. The schematic circuit of the converter module can be seen in Figure-3. It uses an electrical switching circuit with a TL494 as a square signal generator. The signal drives the two NFETs (N type-field effect transistor) to flow the high electrical current to a coil's primary winding. A 12 V DC on the primary winding will be switched. Then, the secondary winding of a conductive wire bobbin will give an AC voltage. After the secondary winding, the bridge circuit will convert to the DC voltage, and the capacitor components will filter a spike DC voltage. Hence, the output will be a pure DC voltage. In short, the module will be active (giving the output voltage) when a 12 V input connects to the REM pin, resulting in the output voltage being about  $\pm 32$  V. The output will be used between the pin of -32 V and +32 V for the maximum application. Hence, the total outcome of a module will be approximately 64 V.

Figure-4 shows the physical image of the converter module and a simplifying block symbol to make the schematic system design more applicable. The advantage of using the isolated DC-to-DC converter module is if a method implements more converter modules, it only needs one battery for the input supply of all modules. The DC power module schematic of a geoelectrical device using the isolated DC to DC converter module is shown in Figure-5.

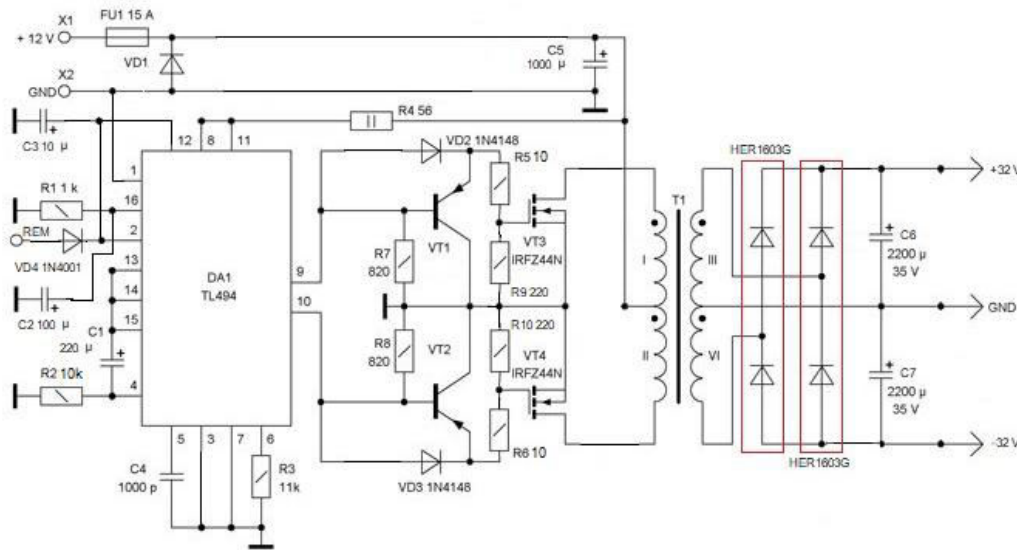


Figure-3. Schematic circuit of a converter module (modified from [33]).

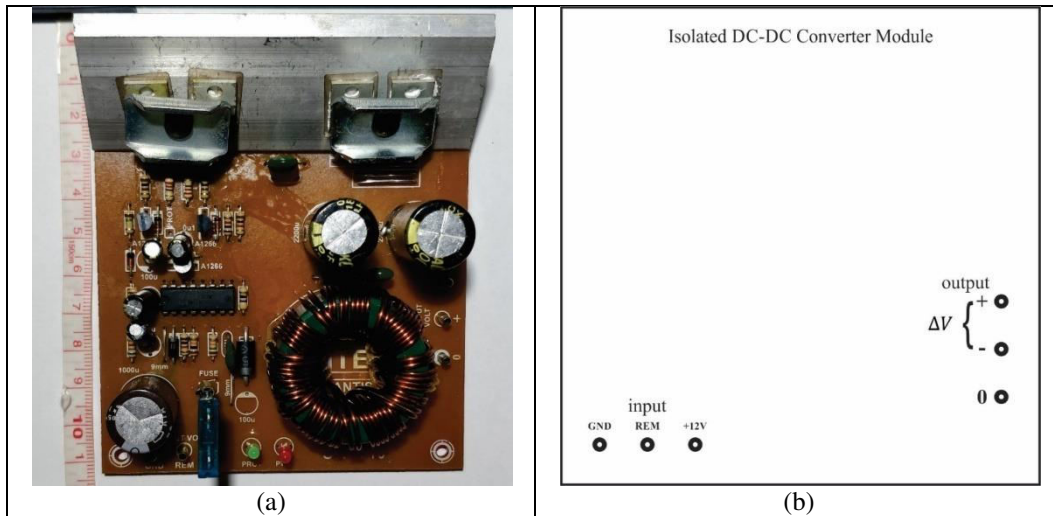


Figure-4. (a) An isolated DC-DC converter module, and (b) A simplifying block symbol of the module.

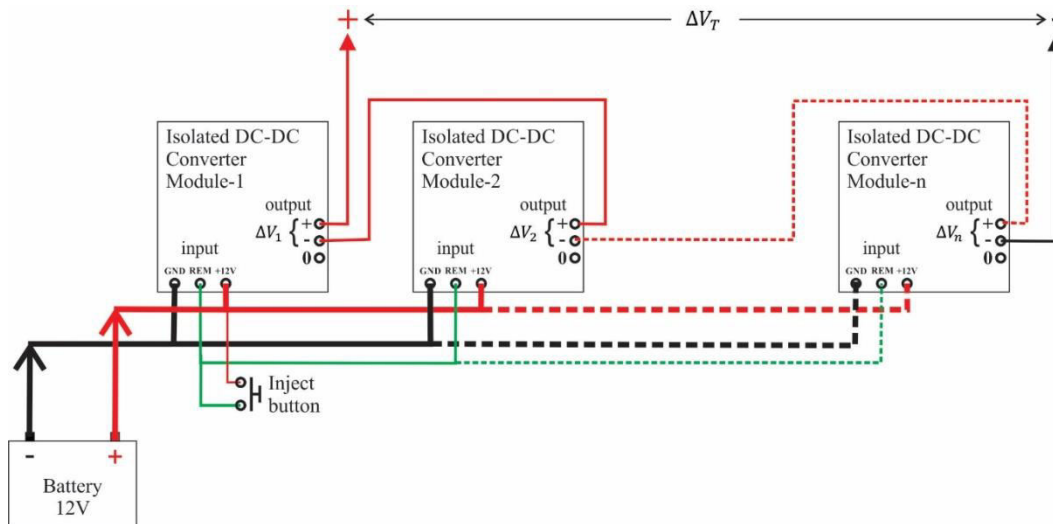


Figure-5. DC power circuit comes from the connection of isolated DC-DC converter modules in series.



The design is similar to Figure-2 in that the battery is replaced by the converter module and an additional part for activating the power module, given by the "Inject button." By modifying Eq. (1), the total output voltage of the module ( $\Delta V_T$ ) in Figure-5 is

$$\Delta V_T = \Delta V_1 + \Delta V_2 + \dots + \Delta V_n \quad (4)$$

with the symbols ( $\Delta V_1$ ,  $\Delta V_2$ , and  $\Delta V_n$ ) are the converter output voltage of the first, the second, and the  $n$ -th, respectively. If each converter module has the same output voltage of  $\Delta V$ , like the following statement

$$\Delta V_1 = \Delta V_2 = \dots = \Delta V_n = \Delta V \quad (5)$$

the total output voltage in Eq. (4) will be

$$\Delta V_T = N_c \Delta V \quad (6)$$

where  $N_c$  is the number of the converter modules.

The design of the DC power module implemented nine converter modules to achieve the target output voltage of about 500 V. For the complete equipment (to be ready to use), the production cost estimation is given in Table 1. The total cost is approximately 350 USD (1 USD = 14,400 IDR) with the following distribution: 150 USD for the DC power

module, 18 USD for the digital meter module, and the rest for the accessories. This DC power module is very inexpensive compared to the previous method. The cost in an earlier approach method is only for the batteries without a case and some connectors. If they are included, it will approximate about 700 USD. That is an additional reason not to apply the previous method. The second method is the best option and is a meager cost. There are two multimeters in the digital meter module, and each multimeter can be an amperemeter or a voltmeter. The type of multimeter is ZT100, an auto-range digital multimeter with a dimension of 130 x 65 x 32 mm [34]. It can measure a voltage value of mV order up to 1,000 V, and the current measurement is from mA order up to 10 A [34].

The accessories contribute the highest cost in this study (Table-1); one of them is the cables. The length of wires depends on the need (target of the research activity). The maximum size of field measurement can be calculated from a distance between  $C_1$  and  $C_2$  (Figure-1). The distance is determined by the maximum length of the cables which are connected to the electrodes  $C_1$  and  $C_2$  (from the central unit). The more extended size of field measurement is, the longer the cable is required. The wires provided in this study have a length of 100 m each (Table 1); thus, the maximum distance is 200 m.

**Table-1.** Cost production of the built geoelectrical equipment.

| Item  | Q   | Unit   | Unit cost <sup>a</sup> (in thousand IDR) | Total item cost (in thousand IDR) |
|---|-----|--------|--|-----------------------------------|
| DC Power Module:                                  |     |        |  | 1,085.3                           |
| Outdoor case (34.5 x 29.5 x 15.4 cm)              | 1   | Piece  | 749                                      | 749                               |
| Isolated DC-DC converter module                   | 9   | Pieces | 65                                       | 585                               |
| Binding post connector                            | 4   | Sets   | 8.5                                      | 34                                |
| Aviation connector                                | 3   | Pieces | 74                                       | 222                               |
| 20 mm PCB spacer                                  | 24  | Pieces | 1.2                                      | 28.8                              |
| Plastic box (100 x 75 x 35 mm)                    | 1   | Piece  | 5.5                                      | 5.5                               |
| Push on button                                    | 1   | Piece  | 2.6                                      | 2.6                               |
| Battery power cable                               | 1   | Set    | 46.9                                     | 46.9                              |
| 8-core cable                                      | 1   | Meter  | 12.5                                     | 12.5                              |
| Cable of 1 mm diameter (for jumper)               | 4   | Meters | 1  | 4                                 |
| 12 V rechargeable battery                         | 1   | Piece  | 260                                      | 260                               |
| 12 V battery charger                              | 1   | Piece  | 135                                      | 135                               |
| Digital meter module:                             |     |        |  | <b>252.5</b>                      |
| Small case (160 x 120 x 70 mm)                    | 1   | Piece  | 35                                       | 35                                |
| Digital multimeter ZT-100                         | 2   | Pieces | 105                                      | 210                               |
| Banana connector (for power module to multimeter) | 2   | Sets   | 3.75                                     | 7.5                               |
| Accessories:                                      |     |        |  | 2,488.5                           |
| Cable of 1 mm diameter (each electrode is 100 m)  | 400 | Meters | 3.9                                      | 1,560                             |
| Spool (for cable roll)                            | 4   | Pieces | 15                                       | 60                                |
| Stainless electrode                               | 4   | Pieces | 150                                      | 600                               |
| Banana connector (for cable to power module)      | 2   | Sets   | 3.75                                     | 7.5                               |
| Alligator connector (for cable to electrode)      | 2   | Sets   | 5  | 10                                |
| Measuring tape                                    | 2   | Pieces | 78                                       | 156                               |
| Hammer  | 2   | Pieces | 47.5                                     | 95                                |
| Total cost (in thousand IDR)                      |     |        |  | 4,826.3                           |

<sup>a</sup>Price was based on July 31, 2021.

### 3. RESULTS AND DISCUSSIONS

Before taking the field data acquisition, simple testing is required to prove that the built geoelectrical equipment is feasible. First, check out the total output voltage of the DC power module. The theoretical calculation employs Eq. (6); each converter module has an output voltage ( $\Delta V$ ) of about 64 V. So, the serial connection of nine converter modules ( $N_c = 9$ ) should

have a total output ( $\Delta V_T$ ) of 576 V. But in fact, the total output of the DC power module was about 517 V (shown in Figure-6(a)). There are a few possibilities that the measured output voltage is smaller than the calculated value: the output voltage of the converter module is not precisely 64 V, and the output voltage is not uniform. When the study was implemented, it did not check the output of each converter module. Even though the measured output voltage is not the same as a theoretical



calculation, the system is good enough (it appropriates the target output design).

Second, the system was tested to measure the electrical resistance of several materials ( $R_{mate}$ ) in a laboratory. Each material has a known value of resistance with a dissipation power ( $P_{diss}$ ) of 20 W (they ( $R_{mate}$ ) were the only available material for the testing, presented in columns 1 and 2 of Table-2). According to Ohm's law, every material has a maximum electrical current ( $I_{max}$ ) that it can accept. The statement can be expressed by

$$I_{max} = \sqrt{\frac{P_{diss}}{R_{mate}}} \tag{7}$$

The calculation of  $I_{max}$  in each material is given in column 3 of Table-2. The output voltage ( $V_{out}$ ) of the DC power module is fixed (about 500 V, shown in column 4 of Table-2). Then, if the material is directly connected to the module output, Ohm's law will apply. The output electrical current ( $I_{out}$ ) of the module will be proportional to the output voltage and inversely proportional to the resistance material, with the following equation

$$I_{out} = \frac{V_{out}}{R_{mate}} \tag{8}$$

The calculation of  $I_{out}$  can be seen in column 5 of Table-2. Theoretically, the value of  $I_{out}$  should be smaller

than  $I_{max}$  because to prevent the material and the module itself from being damaged.

Hence, the measuring method implemented the equivalent circuit of Figure-1, introduced by Antosia [35]. The approach assumed that each electrode interval ( $C_1 - P_1$ ,  $P_1 - P_2$ , and  $C_1 - C_2$ ) is a resistance material (shown in Figure-7). The built instrument measured the resistance value of a material  $R$ . The resistance value of the material ( $R_1$ ) was constant, and the material acted as a current limiter in this testing mode. The method was similar to the actual field data measurement; a resistance material simulates the earth's surface.

**Table-2.** Maximum current calculation based on dissipation power of the resistance material and output current estimation based on the output voltage of the DC power module.

| $R_{mate}$ ( $\Omega$ ) | $P_{diss}$ (W) | $I_{max}$ (A) | $V_{out}$ (V) | $I_{out}$ (A) |
|-------------------------|----------------|---------------|---------------|---------------|
| 1                       | 20             | 4.47          | 500           | 500           |
| 4                       | 20             | 2.24          | 500           | 125           |
| 10                      | 20             | 1.41          | 500           | 50            |
| 20                      | 20             | 1.00          | 500           | 25            |
| 68                      | 20             | 0.54          | 500           | 7.35          |
| 100                     | 20             | 0.45          | 500           | 5             |

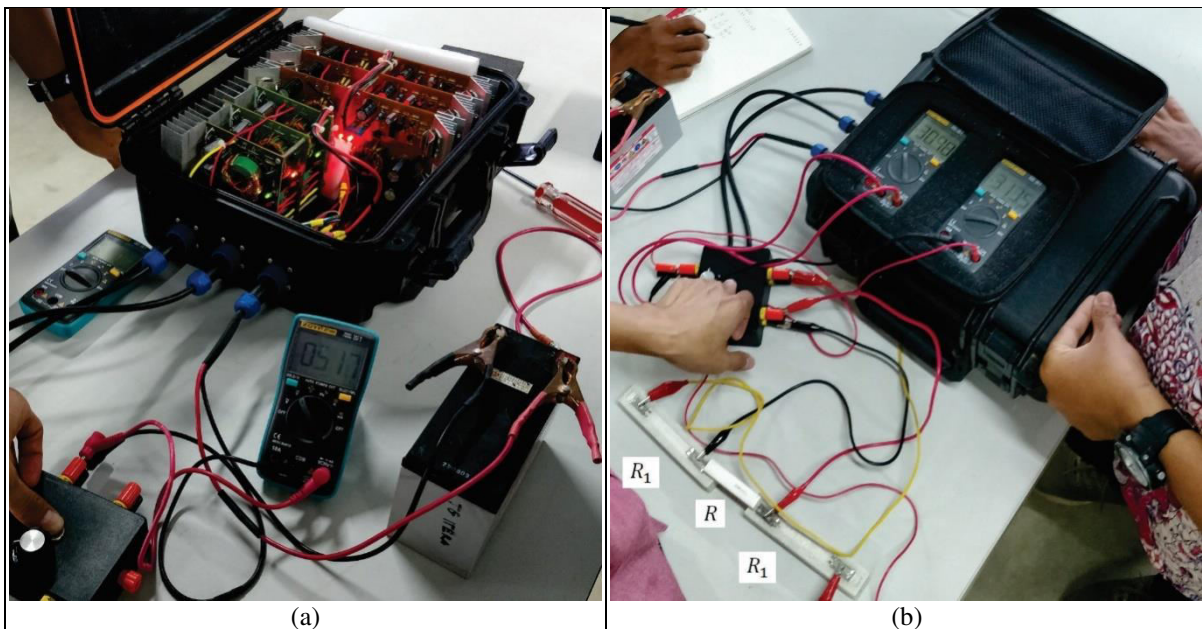


**Figure-6.** Laboratory testing of the built geoelectrical equipment, (a) Testing the DC power module output voltage, and (b) Testing the resistance material refers to Figure-7.

The total resistance value ( $R_T$ ) between  $C_1$  and  $C_2$  is

$$R_T = 2R_1 + R \tag{9}$$

In the laboratory, the availability of material  $R_1$  had a value of 500  $\Omega$  with a dissipation power of 100 W. There are three calculation steps to ease the analysis:

- a) Resistance calculation of the material  $R_T$ . In the equivalent circuit, the material  $R_{mate}$  is the same as  $R$ ; by referring to Eq. (9), the calculated value of  $R_T$  is



$$R_T = 1,001 - 1,100 \Omega \quad (10)$$

b) Maximum current calculation ( $I_{max}$ ) of  $R_1$ . By replacing the material  $R_{mate}$  with  $R_1$  in Eq. (7), the current  $I_{max}$  of  $R_1$  can be obtained (see Eq. (11) for the outcome). Because the equivalent circuit is in series, the maximum electrical current flowing to each resistance material is the same. So, the calculated current will be the smallest one (the current  $I_{max}$  of  $R_1$  is the smallest value compared to the result in column 3 of Table-2)

$$I_{max} = 0.45 \text{ A} \quad (11)$$

c) Output current calculation ( $I_{out}$ ) of the DC power module. By assuming the output voltage of the module is 500 V and replacing the material  $R_{mate}$  with  $R_T$  in Figure-7, then applying equations (8) and (10), the output current is

$$I_{out} = 0.46 - 0.50 \text{ A} \quad (12)$$

The calculated current  $I_{out}$  is slightly higher than  $I_{max}$  but the difference is about 0.01-0.05 A (better than the difference presented in columns 3 and 5 of Table-2). The author thinks it is still safe because the material resistance will only be warm or even hot for the short term, not damaged.

Figure-6(b) gives a brief illustration of the testing. The testing outcomes are shown in Table-3. The multimeter ZT100 can also be an ohmmeter [34]. It is applied to measure the known resistance to get the actual value ( $R_{meas}$ ). The measured values in a geoelectrical instrument are a voltage difference between  $P_1$  and  $P_2$  ( $V_{meas}$ ) and an electrical current ( $I_{meas}$ ) flowing to the material resistance. Ohm's law will also apply to the calculation of the resistance value with the following equation

$$R_{calc} = \frac{V_{meas}}{I_{meas}} \quad (13)$$

Then, to ensure the calculated value ( $R_{calc}$ ) is close to the measured value ( $R_{meas}$ ), the misfit calculation ( $e_{calc}$ ) is required; here is the equation

$$e_{calc} = \left| \frac{R_{calc} - R_{meas}}{R_{meas}} \right| \times 100\% \quad (14)$$

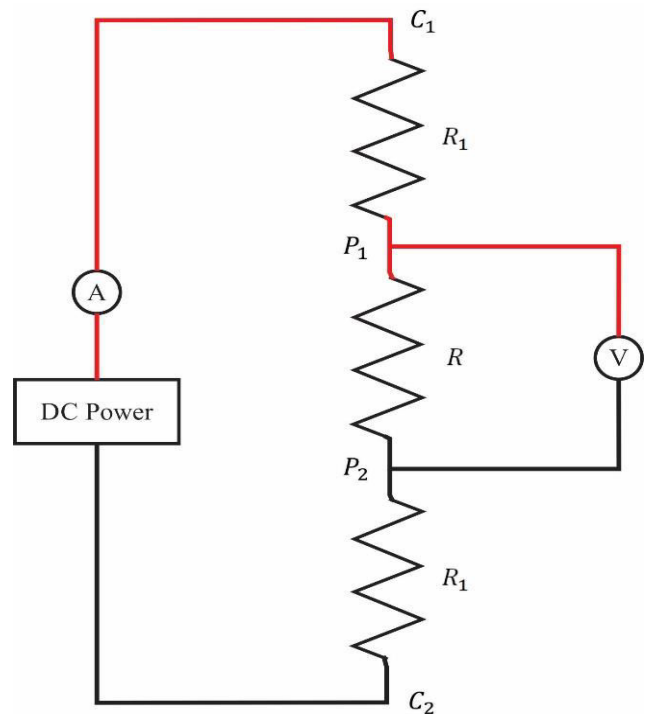


Figure-7. An equivalent circuit of Figure-1 for testing mode in a laboratory (modified from Antosia [35]).

Table-3. Laboratory testing data of the built geoelectrical instrument.

| 20W<br>$R_{mate}$ ( $\Omega$ ) | $R_{meas}$ by ZT-100 ( $\Omega$ ) | The built geoelectrical instrument |                 |                         |                |
|--------------------------------|-----------------------------------|------------------------------------|-----------------|-------------------------|----------------|
|                                |                                   | $V_{meas}$                         | $I_{meas}$ (mA) | $R_{calc}$ ( $\Omega$ ) | $e_{calc}$ (%) |
| 1                              | 0.9                               | 313.4 mV                           | 332.0           | 0.94                    | 4.89           |
| 4                              | 3.8                               | 1.216 V                            | 332.0           | 3.66                    | 3.61           |
| 10                             | 10                                | 3.317 V                            | 331.8           | 9.99                    | 0.03           |
| 20                             | 20.1                              | 6.670 V                            | 336.7           | 19.81                   | 1.44           |
| 68                             | 69                                | 21.54 V                            | 318.1           | 67.71                   | 1.86           |
| 100                            | 99.5                              | 31.50 V                            | 319.3           | 98.65                   | 0.86           |

Based on Table-3, the calculated resistance has a maximum misfit of about 5% to the measured resistance. The confidence level is excellent; the minimum level is about 95%. In general, the material resistance that the dissipation power is greater than or equal to 5 W has a tolerance level of 10%. Thus, the testing gives a good outcome; it is at the tolerance level of the material.

Theoretically, the output current of the system should be following the calculation in Eq. (11), but the measured value is around 0.3 A (column 4 of Table-3). The possibility is the system's output voltage had dropped due to the total resistance value of the load ( $R_T$ ) was too large. The author thinks it does not matter because the testing has two aims: to measure  $V_{meas}$  and  $I_{meas}$  values, then



calculate the value of  $R_{calc}$  (also compared to the value of  $R_{meas}$ ); to ensure that the material  $R_T$  and the system will not be damaged.

The third is the comparison of field testing between the commercial and the built equipment. The measurement method refers in Figure-1, with the interval of each electrode being one meter. The testing used the same accessories to give a reliable data comparison. Table 4 presents the outcome. When this study was conducted, the output voltage of the commercial instrument had not been checked; it might be around 500-600 V. The location of the field testing was the same, so the resistance value should also be the same. Repeated measurement up to three times was carried out to ensure the consistency of the

calculated resistance. Each instrument's estimated resistance value (using Eq. (13)) is compared; the difference is about one Ohm. This result shows that the built system is perfect; it is ready for actual field data acquisition.

The presented data in Table-4 shows that the commercial equipment gives a higher voltage and current response than the built equipment. The commercial instrument might have a greater output power than the built instrument. Because of the limited facilities in a laboratory, this study could not carry out the output power measurement. It needs an adjustable resistance device with considerable dissipation power. It can provide from a low to a high resistance value.

**Table-4.** Field testing data comparison of geoelectrical device.

| The commercial geoelectrical device |                 |                         | The built geoelectrical device |                 |                         |
|-------------------------------------|-----------------|-------------------------|--------------------------------|-----------------|-------------------------|
| $V_{meas}$ (mV)                     | $I_{meas}$ (mA) | $R_{calc}$ ( $\Omega$ ) | $V_{meas}$ (V)                 | $I_{meas}$ (mA) | $R_{calc}$ ( $\Omega$ ) |
| 5,270                               | 510             | 10.333                  | 4.920                          | 435             | 11.310                  |
| 5,290                               | 511             | 10.352                  | 4.930                          | 435             | 11.307                  |
| 5,280                               | 510             | 10.353                  | 4.920                          | 435             | 11.310                  |

There was another way to know the output power of the built system. In the field testing, the arrangement of the electrodes referred to Rizka & Satiawan [3] and Igboama & Ugwu [18], who had deployed the minimum electrode interval of one meter. In this study, the author assumed that the earth's resistance has an enormous dissipation power; and with such configuration, the system will measure the minimum resistance value in the field. If the material  $R_{mate}$  is the same as the field minimum resistance, according to Eq. (8), with a fixed value of  $V_{out}$  (assume the output voltage  $V_{out}$  is the maximum output  $V_{o-max}$ ), the output current  $I_{out}$  will be maximum ( $I_{(o-max)}$ ). The total output power ( $P_{o-max}$ ) of the built instrument can be calculated by applying the following equation

$$P_{o-max} = (V_{o-max})(I_{o-max}) \quad (15)$$

The configuration of the field testing was as though the serial connection (see the equivalent circuit). So, the maximum output current ( $I_{o-max}$ ) would be equal to the measured current ( $I_{meas}$ ). The maximum outcomes of voltage and current were approximately 500 V and 0.4 A (the average current value in column 5 of Table-4). Therefore, the output power ( $P_{o-max}$ ) of the built equipment was estimated at 200 W (using Eq. (15)).

Finally, the built system's actual field data acquisition was carried out. The field measurement was a case study identifying the aquifer with only one sounding point of a 1-D geoelectrical method with a Schlumberger array (the technique referred to Rizka & Satiawan [3]). Near the point, there were two wells with different groundwater levels. The first groundwater well had a depth of about three-meter, and the second had a groundwater level of about 32 m. The distance from the

sounding point to the first well was estimated at 20 m, and the other was about 40 m. The coordinate points of the location can be seen in Table-5.

**Table-5.** Sounding point and groundwater well coordinates.

| Name               | Latitude  | Longitude  |
|--------------------|-----------|------------|
| Sounding Point     | -5.338439 | 105.343266 |
| Groundwater well 1 | -5.338565 | 105.343390 |
| Groundwater well 2 | -5.338538 | 105.342915 |

The maximum length of the data acquisition was 200 m (see the previous explanation about the cables). So, the maximum distance of half interval  $C_1 - C_2$  was 100 m (see column 1 of Table-6). The observed data in Table 6 has a good value; which can be seen in the measured voltage and current values ( $V_{meas}$  and  $I_{meas}$ ). There was a set measurement limit; namely, the measured values should not be less than 5 mV and 5 mA; because the author thinks if the value is less than the set limit, the data is too noisy. But even though the last measured voltage is less than 5 mV, it is still reasonable due to the data trend before.

Figure-8(a) shows the data processing result from the observed data in Table-6. The aim is to get the resistivity and depth estimations of the earth's layer (vertically at the sounding point). The location has the same geological formation (it is still in one geological region) as the study area of Rizka & Satiawan[3]. By treating both locations with uniformity of the earth's layer, interpreting the data processing result can implement the resistivity outcomes of Rizka & Satiawan [3].



**Table-6.** Field data acquisition of 1-D geoelectrical method with Schlumberger array.

| $\frac{1}{2}C_1C_2$<br>(m) | $\frac{1}{2}P_1P_2$ (m) | $V_{meas}$ | $I_{meas}$ (mA) |
|----------------------------|-------------------------|------------|-----------------|
| 3                          | 0.5                     | 0.423 V    | 108             |
| 5                          | 0.5                     | 223.9 mV   | 141             |
| 6                          | 0.5                     | 53.5 mV    | 55              |
| 6                          | 2                       | 256.1 mV   | 58              |
| 8                          | 2                       | 299.9 mV   | 154             |
| 10                         | 2                       | 219.7 mV   | 205             |
| 15                         | 2                       | 50.9 mV    | 114             |
| 20                         | 2                       | 24.5 mV    | 89              |
| 20                         | 10                      | 159.6 mV   | 89              |
| 30                         | 10                      | 54.4 mV    | 63              |
| 40                         | 10                      | 35.9 mV    | 67.5            |
| 50                         | 10                      | 16.1 mV    | 47              |
| 60                         | 10                      | 36.3 mV    | 151.8           |
| 80                         | 10                      | 14.6 mV    | 123             |
| 100                        | 10                      | 3.1 mV     | 51              |

The following explanation is a short description of the data processing result in Figure-8(a). A forward modelling process generates the calculated information (see Heriyanto & Srigutomo [36] and Farduwin *et al.* [37]

for a more detailed description). A good outcome in estimating resistivity and depth values can be seen if the observed and calculated data are fitted well, producing a minimum error. The impact is shown in Fig. 8(a) has a minimum error of about 5% (or the confidence level approximates about 95%). Thus, the estimation values are well-turned.

To conveniently analyze, a log value per depth (Figure-8(b)) is produced with the information of the estimated layer according to Rizka & Satiawan [3]. They said that the aquifer in the study area is tuffaceous sand. The interpretation matches the depth of the groundwater wells. The first tuffaceous sand is at about 2.9 m (layer no. 3 in Figure-8(b)), while the first groundwater depth is at three-meter; thus, the result is fitted well. Meanwhile, the second groundwater depth is 32 m, and the second tuffaceous sand is approximately 28 m (layer no. 5 in Figure-8(b)); the result is not matched well, but it is still at the estimated aquifer. Despite the sounding point and the groundwater wells being at the same elevation, there is the possibility that the depth of the earth's subsurface layer is not the same. It might argue for the level difference between the second aquifer and the second well. The outcome also provides the estimated thickness of the aquifer (Figure-8(b)). The first aquifer has a thickness of about five-meter. The second has an unknown thickness (it is called half-space [36, 37]) due to the depth penetration being at a limit (need a more extended measurement for the deeper penetration). There is a correlation between the measurement length and the maximum depth penetration [38]. It is common in the 1-D geoelectrical data processing that the bottom layer has an unknown thickness.

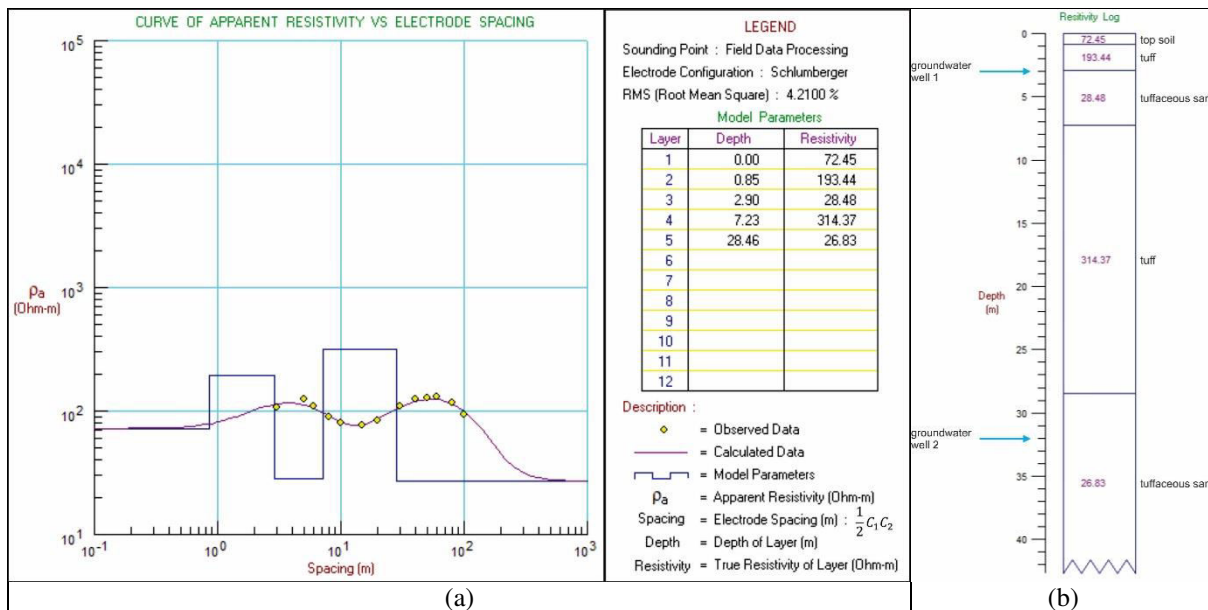


**Figure-8.** (a) Result of field data processing and (b) Resistivity data interpretation.

**4. CONCLUSIONS**

The built geoelectrical equipment used the local component to achieve a low-cost production (estimated at 350 USD). The primary unit cost about 170 USD, and the

rest was for the accessories. The instrument had a sound design. It was easy to assemble because of using the minimum components. The DC power module of the built device implemented nine isolated converter modules,



which a total output voltage of about 500 V; the maximum output power was approximately about 200 W. The laboratory testing has a good result with a confidence level of about 95%. Later, the field testing was conducted; and the built system impact was close to the commercial one. Then, there was a case study to spot the aquifer. It was an actual field data acquisition to prove that the equipment was ready to apply. Based on the field data processing outcome, the depth aquifer interpretation is well-matched with the information on groundwater wells.

For further development, some adjustments are required:

- a) Install a protection circuit or an automatic fuse to the output system to prevent a short circuit from being damaged.
- b) Develop a digital design (replace the multimeters with the built digital meter) using the introduced method by Antosia [35] because he has considered the possibility of the reversed polarity measurement; it can also be applied for the Induced Polarization development.
- c) Implement a switched polarity circuit to the output power (likely most commercial instruments employ it), exemplified by Indarto et al. [24]. It aims to minimize the polarity effect of injecting electrical current into the earth's subsurface.

#### ACKNOWLEDGEMENTS

The author would like to express his gratitude to the students of Geophysical Engineering-Institut Teknologi Sumatera for assisting the data collection and the field data acquisition.

#### Conflict of Interests

The author did not receive any sponsorship to carry out the research reported in the present manuscript. There is no direct or indirect conflict of interest related to the subject of the work.

#### REFERENCES

- [1] Ahmad M. N., Iqbal F., Maqbool S. and Arshad M. B. 2019. Low-Cost Resistivity Meter for Groundwater Exploration Using High Voltage Experimentations. *International Journal of Economic and Environmental Geology*, 10(3): 35-39. <https://doi.org/10.46660/ijeeg.vol10.iss3.2019.306>
- [2] Asta and Prasetya A. M. 2020. Application of Vertical Electrical Sounding (VES) Method with Resistivity Meter Based on Boost Converter to Estimate the Potential of Groundwater Aquifers in KarangAnyar of Tarakan City. *MATEC Web of Conferences*, 331, 06001. <https://doi.org/10.1051/mateconf/202033106001>
- [3] Rizka and Satiawan S. 2019. Investigasi Lapisan Akuifer Berdasarkan Data Vertical Electrical Sounding (VES) dan Data Electrical Logging; Studi Kasus Kampus ITERA. *Bulletin of Scientific Contribution: Geology*, 17(2): 91-100. <https://doi.org/10.24198/bsc%20geology.v17i2.22393>
- [4] Olanrewaju A. A., Nafiu A. K. A. and Oluwole O. G. 2020. Fabrication of resistivity meter and its evaluation within shallow depth of investigation. *Global Journal of Engineering and Technology Advances*, 04(01): 015-029. <https://doi.org/10.30574/gjeta.2020.4.1.0042>
- [5] Urang J. G., Awak E. A. and Bamidele A. S. 2018. Design and construction of a simple resistivity meter for resistivity measurement. *Research Journal of Physical Sciences*. 6(5): 1-7.
- [6] Prasetya A. M., Aidil R. and Faizal R. 2018. Penggunaan Resistivity Meter Berbasis Boost Converter untuk Identifikasi Batuan Dasar Pancang Pondasi Bangunan di Pulau Tarakan. *Borneo Engineering: Jurnal Teknik Sipil*, 2(2): 127-136. <https://doi.org/10.35334/be.v2i2.620>
- [7] Antosia R. M., Mustika Putri I. A., Rasimeng S. and amp Dinata O. 2021. Andesite prospect at West Sungkai of North Lampung: Its distribution based on electrical resistivity tomography. *IOP Conference Series: Earth and Environmental Science*, 882(1): 012086. <https://doi.org/10.1088/1755-1315/882/1/012086>
- [8] Yogi I. B., Pangestu R., Karyanto K. and Darmawan I. G. 2020. Instrumen Real Time Rock Resistivity Meter untuk Mengukur Resistivitas dan Memonitor Sifat Kelistrikan Sampel Batuan. *Jurnal Geosaintek*, 6(3): 143-152. <https://doi.org/10.12962/j25023659.v6i3.7890>
- [9] Acho L., Pujol-Vázquez G. and Gibergans-Báguena J. 2021. Electronic Device and Data Processing Method for Soil Resistivity Analysis. *Electronics*, 10(11): 1281. <https://doi.org/10.3390/electronics10111281>
- [10] Fatahillah D., Darsono and Nuryani N. 2019. Low-cost multi electrode resistivity meter based on microcontroller for electric resistivity tomography purpose. *Journal of Physics: Conference Series*, 1153,



012022. <https://doi.org/10.1088/1742-6596/1153/1/012022> 7(3): 179-190. <https://doi.org/10.3997/1873-0604.2009011>

- [11] Irvan A., Nehru and Samsidar. 2019. Digitalisasi Alat Geolistrik Untuk Konfigurasi Schlumberger Berbasis Pengendali Mikro Arduino Mega. *Journal Online of Physics*, 4(2): 15-19. <https://doi.org/10.22437/jop.v4i2.6000>
- [12] Juhari K. N., Noor N. M., Jusoh M. H., Hussin M. F. and Sulaiman A. A. 2016. The Development of a Small Range Soil Electrical Resistivity Meter Based on Wenner Configuration. *International Journal of Simulation: Systems, Science & Technology*, 17(41): 9.1-9.6. <https://doi.org/10.5013/ijssst.a.17.41.09>
- [13] Meraz J. S., Fernandez F. and Magana, L. F. 2009. Electrolytic resistivity measurement using alternating current with high frequencies. *Revista Mexicana De Fisica*. 55(2): 149-152.
- [14] Setiadi I. C. 2015. Desain Sumber Arus untuk Electrical Impedance Tomography (EIT). *Jurnal Arus Elektro Indonesia*. 1(3): 27-33.
- [15] Toll D. G. and Hassan A. 2014. Data Acquisition and Control Software for Automated Resistivity Measurements. *Information Technology in Geo-Engineering*, 3, 170-176. <https://doi.org/10.3233/978-1-61499-417-6-170>
- [16] Yohandri Mairizwan and Akmam. 2018. Development of a Digital Resistivity Meter Based on Microcontroller. *TENCON 2018 - 2018 IEEE Region 10 Conference*, 0551-0554. <https://doi.org/10.1109/tencon.2018.8650464>
- [17] Ibitola G. A., Emmanuel O. A., Ajanaku O. and Ilori A. O. 2019. Design, Construction and Performance Evaluation of Soil Resistivity Meters at Six Geophysical Sites in Osustech, Okitipupa - Nigeria. *International Journal of Geoinformatics and Geological Science*, 6(3): 24-30. <https://doi.org/10.14445/23939206/IJGGS-V6I3P104>
- [18] Igboama W. and Ugwu N. 2011. Fabrication of resistivity meter and its evaluation. *American Journal of Scientific and Industrial Research*, 2(5): 713-717. <https://doi.org/10.5251/ajsir.2011.2.5.713.717>
- [19] Gebbers R., Lück E., Dabas M. and Domsch H. 2009. Comparison of instruments for geoelectrical soil mapping at the field scale. *Near Surface Geophysics*, 7(3): 179-190. <https://doi.org/10.3997/1873-0604.2009011>
- [20] PDDikti. 2020a. Pangkalan Data Pendidikan Tinggi Search Result for: kebumian. Pangkalan Data Pendidikan Tinggi. Retrieved May 2, 2022, from <https://pddikti.kemdikbud.go.id/search/kebumian>
- [21] PDDikti. 2020b. Pangkalan Data Pendidikan Tinggi Search Result for: geofisika. Pangkalan Data Pendidikan Tinggi. Retrieved May 2, 2022, from <https://pddikti.kemdikbud.go.id/search/geofisika>
- [22] PDDikti. 2020c. Pangkalan Data Pendidikan Tinggi Search Result for: geologi. Pangkalan Data Pendidikan Tinggi. Retrieved May 2, 2022, from <https://pddikti.kemdikbud.go.id/search/geologi>
- [23] PDDikti. 2020d. Pangkalan Data Pendidikan Tinggi Search Result for: geografi. Pangkalan Data Pendidikan Tinggi. Retrieved May 2, 2022, from <https://pddikti.kemdikbud.go.id/search/geografi>
- [24] Indarto B., Sudenasahaq G. R. F., Rachmad D. B., Basri M. H. and Sunarno H. 2016. Rancang Bangun Sistem Pengukuran Resistivitas Geolistrik dengan menggunakan Sumber Arus Konstan. *Jurnal Fisika Dan Aplikasinya*, 12(2): 83-89. <https://doi.org/10.12962/j24604682.v12i2.1336>
- [25] Maison Sawitri K. N., Samsidar Handayani L., Purbakawaca R. and Nurjaman J. 2019. Design of digital resistivity-meter for subsurface exploration. *Journal of Physics: Conference Series*, 1282, 012051. <https://doi.org/10.1088/1742-6596/1282/1/012051>
- [26] Imaduddi I., Srigutomo W. and Mustopa E. J. 2019. Development of Data Acquisition Instrumentation and Inversion System for Earth Resistivity Survey in a Smart Integrated System, *Journal of Physics: Conference Series*, 1204(2019): 012122. <https://doi.org/10.1088/1742-6596/1204/1/012122>
- [27] AGI. 2021. MiniSting™ R1. AGIUSA. Retrieved March 2, 2022, from <https://www.agiusa.com/ministhing>.
- [28] Geotech. 2021. Resistivity system OMEGA-48. Geotech. Retrieved March 2, 2022, from <https://geotechru.com/resistivity-system-omega-48/>.
- [29] IRIS. 2021. Syscal Kid Switch. Retrieved March 2, 2022, from <http://www.iris-instruments.com/syscal-kidsw.html>.



- [30] Landviser. 2016. SibER - multi-electrode resistivity surveying set. SibER - multi-electrode resistivity surveying set | Landviser, LLC. Retrieved March 2, 2022, from <http://www.landviser.net/content/siber-multi-electrode-resistivity-surveying-set>.
- [31] Telford W. M., Geldart L. P. and Sheriff R. E. 1990. Applied Geophysics Second Edition. Cambridge: Cambridge University Press.
- [32] Power Stream. 2021. Sealed Lead Acid Battery Size Chart. Industry standard sealed lead acid battery size and VRLA charts. Retrieved March 2, 2022, from [https://www.powerstream.com/Size\\_SLA.htm](https://www.powerstream.com/Size_SLA.htm)
- [33] PSU. 2011. Car amplifier power supply. Power Supply Circuits. Retrieved March 2, 2022, from <https://powersupply33.com/dc-to-dc-converter-12-v-to-%C2%B138-v.html/car-amplifier-power-supply>
- [34] Zotek. 2021. 4000 Counts Digital Multimeter + Widescreen + Palm Size Multimeter+200 $\mu$ F Capacitance. Zoyi. Retrieved March 2, 2022, from <https://zotektools.com/products/zt-100/>
- [35] Antosia R. M. 2020. Voltmeter Design Based on ADS1115 and Arduino Uno for DC Resistivity Measurement. JTERA (Jurnal Teknologi Rekayasa), 5(1): 73-80. <https://doi.org/10.31544/jtera.v5.i1.2019.73-80>
- [36] Heriyanto M. and Srigutomo W. 2017. 1-D DC Resistivity Inversion using Singular Value Decomposition and Levenberg-Marquardt's Inversion Schemes. Journal of Physics: Conference Series, 877, 012066. <https://doi.org/10.1088/1742-6596/877/1/012066>
- [37] Farduwin A., Antosia R. M., Putri I. A., Santoso N. A. and Irawati S. M. 2021. Inversi Data Geolistrik Menggunakan Particle Swarm Optimization: Studi Kasus Desa Gayau. Jurnal Geofisika Eksplorasi, 7(2): 88-99. <https://doi.org/10.23960/jge.v7i2.118>
- [38] Okpoli C. C. 2013. Sensitivity and resolution capacity of electrode configurations. International Journal of Geophysics, 1-12. <https://doi.org/10.1155/2013/608037>